Au-CdS Core−Shell Nanocrystals with Controllable Shell Thickness and Photoinduced Charge Separation Property

Wei-Ta Chen, Ting-Ting Yang, and Yung-Jung Hsu*

Department of Materials Science and Engineering, National Chiao Tung University, Hsinchu, Taiwan 30010, Republic of China

Received July 29, 2008
Revised Manuscript Received October 19, 2008

Semiconductor, magnetite, or metal-based composite nanocrystals have attracted increasing research attention in recent years for their possible improvement in optical,[1] electronic,[2] magnetic,[3] and catalytic[4] functionalities. In particular, great progress has been made in creating core−shell heterostructures by assembling both metal and semiconductor nanocrystals. Such metal/semiconductor combination is of particular interest to photocatalytic[5] and electron storage applications.[6] For metal−semiconductor core−shell nanocrystals, the presence of the metal−semiconductor interface may promote effective charge carrier transfers to favor charge separation and subsequent photocatalysis.[7] In addition, the semiconductor shell can protect the metal core from chemical poisoning (the hole- or hydroxyl radical-mediated oxidation decomposition) as exposed to the surrounding medium.[8] Metals usually suffer from much serious oxidation since they possess higher oxidation potentials. Embedding metals into semiconductors could reasonably alleviate the chemical poisoning and thus extend the lifetime of the metal/semiconductor composite nanocrystals during their photocatalytic operation.

Most of the semiconductor photocatalysts possess wide band gaps, which can only be operated under ultraviolet irradiation.[9] Much effort has thus been expended to create photocatalysts that respond to visible light, which is much abundant in the solar spectrum. CdS is one of the most attractive visible-light-driven photocatalysts because of its suitable band gap (2.5 eV) corresponding well with the spectrum of sunlight. Furthermore, its valence band at relatively negative potential offers CdS good photocatalytic activities.[10] In this communication, we report a facile and reproducible method for fabrication of Au-CdS core−shell nanocrystals with controllable shell thickness. We analyzed various aspects of the synthetic approach, discussed the optical properties and demonstrated the photoinduced charge separation occurring in the as-synthesized core−shell nanocrystals. The growth of CdS shell on Au nanoparticles involved the binding of L-cysteine−Cd^{2+} (Cys/Cd) complexes toward Au nanoparticles, followed by the decomposition of Cys/Cd and subsequent growth of CdS onto the surfaces of Au. L-Cysteine (Cys), possessing three functional groups (SH, COOH, NH_2), used to be the sulfur source and reaction stabilizer for the growth of sulfide nanocrystals.[11] In the current synthetic system, Cys provided thiol groups that could form fairly stable Cys/Cd complexes with Cd^{2+} ions,[12] amine groups that coupled Cys/Cd complexes with Au,[13] and carboxyl groups promoting the dispersion of Au colloids for the later successful growth of CdS shell.

First, Au colloids with an average diameter of 15 nm were prepared by the citrate reduction method.[14] These citrate-protected Au particles (denoted as Au-Cit) were then coupled with Cys/Cd complexes through the linkage between Au atoms and amine groups of Cys.[13] This coupling event can be confirmed by the formation of nitride constituent (Au−N bonds) observed in the XPS analysis (see the Supporting Information, Figure S1a). Cys/Cd-coupled Au nanoparticles (denoted as Au-(Cys/Cd)) showed considerable stability when dispersed in water, attributable to the electrostatic repulsion between the negatively charged carboxyl groups of Cys at the surfaces of Au (see the Supporting Information, Figure S1b). The stable dispersion of Au-(Cys/Cd) suspension was crucial to the later growth of CdS shell. Noted that Cys/Cd complexes were obtained by adding Cd^{2+} ions in Cys solution (5 mM) in a 1:0.5 molar ratio of Cys:Cd^{2+}. Further increase in Cd^{2+} amount when preparing Cys/Cd complexes caused a serious aggregation of the subsequent Au-(Cys/Cd) colloids, probably because of

* Corresponding author. E-mail: yhsu@cc.nctu.edu.tw.

(1) (a) Liz-Marzán, L. M. *Langmuir* **2006**, *22*, 32. (b) Scholes, G. D. *Adv. Funct. Mater.* **2008**, *18*, 1157.
(2) (a) Lee, J.-S.; Shevchenko, E. V.; Talapin, D. V. *J. Am. Chem. Soc.* **2008**, *130*, 9673. (b) Ghosh, B.; Sahu, S.; Pal, A. J. *J. Phys. Chem. C* **2008**, *112*, 11290. (c) Gooding, A. K.; Gómez, D. E.; Mulvaney, P. *ACS Nano* **2008**, *2*, 669.
(3) (a) Salgueiriño-Maceira, V.; Correa-Duarte, M. A.; Spasova, M.; Liz-Marzán, L. M.; Farle, M. *Adv. Funct. Mater.* **2006**, *16*, 509. (b) Jeong, U.; Teng, X.; Wang, Y.; Yang, H.; Xia, Y. *Adv. Mater.* **2007**, *19*, 33. (c) Salgueiriño-Maceira, V.; Correa-Duarte, M. A. *Adv. Mater.* **2007**, *19*, 4131.
(4) (a) Kamat, P. V. *J. Phys. Chem. C* **2007**, *111*, 2834. (b) Glaspell, G.; Hassan, H. M. A.; Elzatahry, A.; Abdalsayed, V.; El-Shall, M. S. *Top. Catal.* **2008**, *47*, 22.
(5) (a) Dawson, A.; Kamat, P. V. *J. Phys. Chem. B* **2001**, *105*, 960. (b) Kamat, P. V. *J. Phys. Chem. B* **2002**, *106*, 7729. (c) Hirakawa, T.; Kamat, P. V. *J. Am. Chem. Soc.* **2005**, *127*, 3928.
(6) (a) Oldfield, G.; Ung, T.; Mulvaney, P. *Adv. Mater.* **2000**, *12*, 1519. (b) Hirakawa, T.; Kamat, P. V. *Langmuir* **2004**, *20*, 5645. (c) Sakai, H.; Kanda, T.; Shibata, H.; Ohkubo, T.; Abe, M. *J. Am. Chem. Soc.* **2006**, *128*, 4944.
(7) (a) Subramanian, V.; Wolf, E. E.; Kamat, P. V. *J. Phys. Chem. B* **2003**, *107*, 7479. (b) Jakob, M.; Levanon, H.; Kamat, P. V. *Nano Lett.* **2003**, *3*, 353. (c) Subramanian, V.; Wolf, E. E.; Kamat, P. V. *J. Am. Chem. Soc.* **2004**, *126*, 4943.
(8) (a) Subramanian, V.; Wolf, E.; Kamat, P. V. *J. Phys. Chem. B* **2001**, *105*, 11439. (b) Subramanian, V.; Wolf, E. E.; Kamat, P. V. *Langmuir* **2003**, *19*, 469. (c) Lahiri, D.; Subramanian, V.; Shibata, T.; Wolf, E. E.; Bunker, B. A.; Kamat, P. V. *J. Appl. Phys.* **2003**, *93*, 2575.
(9) (a) Lee, J.-C.; Sung, Y.-M.; Kim, T. G.; Choi, H.-J. *Appl. Phys. Lett.* **2007**, *91*, 113104. (b) Wang, Y.; Wang, Y.; Meng, Y.; Ding, H.; Shan, Y.; Zhao, X.; Tang, X. *J. Phys. Chem. C* **2008**, *112*, 6620. (c) Jagadale, T. C.; Takale, S. P.; Sonawane, R. S.; Joshi, H. M.; Patil, S. I.; Kale, B. B.; Ogale, S. B. *J. Phys. Chem. C* **2008**, *112*, 14595.
(10) Bao, N.; Shen, L.; Takata, T.; Domen, K. *Chem. Mater.* **2008**, *20*, 110.
(11) (a) Tong, H.; Zhu, Y.-J.; Yang, L.-X.; Li, L.; Zhang, L.; Chang, J.; An, L.-Q.; Wang, S.-W. *J. Phys. Chem. C* **2007**, *111*, 3893. (b) Xiong, S.; Xi, B.; Xu, D.; Wang, C.; Feng, X.; Zhou, H.; Qian, Y. *J. Phys. Chem. C* **2007**, *111*, 16761. (c) Xiang, J.; Cao, H.; Wu, Q.; Zhang, S.; Zhang, X.; Watt, A. A. R. *J. Phys. Chem. C* **2008**, *112*, 3580.
(12) (a) Xiong, S.; Xi, B.; Wang, C.; Zou, G.; Fei, L.; Wang, W.; Qian, Y. *Chem.—Eur. J.* **2007**, *13*, 3076. (b) Zhao, P.; Huang, K. *Cryst. Growth Des.* **2007**, *8*, 717.
(13) (a) Yang, Y.; Shi, J.; Chen, H.; Dai, S.; Liu, Y. *Chem. Phys. Lett.* **2003**, *370*, 1. (b) Sheeney-Haj-Ichia, L.; Pogorelova, S.; Gofer, Y.; Willner, I. *Adv. Funct. Mater.* **2004**, *14*, 416.
(14) (a) Turkevich, J.; Hillier, J.; Stevenson, P. C. *Discuss. Faraday Soc.* **1951**, *11*, 55. (b) Ji, X.; Song, X.; Li, J.; Bai, Y.; Yang, W.; Peng, X. *J. Am. Chem. Soc.* **2007**, *129*, 13939.

10.1021/cm802074j CCC: $40.75
Published on Web 11/14/2008

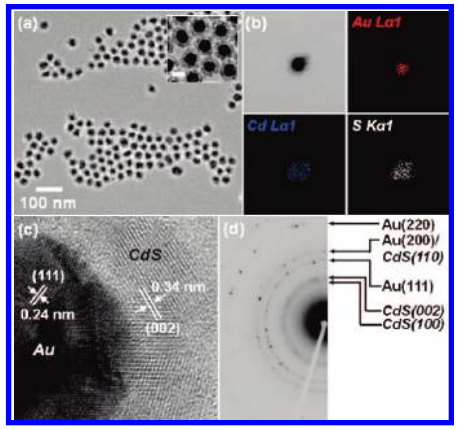

Figure 1. Au-CdS nanocrystals prepared with a Cys/Cd concentration of 5 mM: (a) low-magnification TEM images; (b) TEM-EDS elemental mapping taken on a single core−shell particle; (c) HRTEM image; and (d) the corresponding SAED pattern of a single core−shell particle. The scale bar of the inset in (a) is 20 nm.

the pronounced coupling effect between Cd^{2+} and carboxyl groups of Cys and thus the loss of electrostatic stabilization. Figure S2 in the Supporting Information compares the UV−visible spectra of Au-(Cys/Cd) colloids prepared with various Cys:Cd^{2+} ratios. As compared to Au-Cit colloids, Au-(Cys/Cd) with a Cys:Cd^{2+} ratio of 1:0.5 showed a slight but not significant variation in their surface plasmon resonance (SPR) absorption characteristics. An additional absorption band at longer wavelength was however observed for Au-(Cys/Cd) when the ratio of Cys:Cd^{2+} was increased to 1:0.8. The presence of the long-wavelength absorption band implies that either Au particles agglomerate to some extent or a significant change in the surface chemistry of Au occurs.[15] We attribute the long-wavelength absorption band of Au-(Cys/Cd) colloids to the aggregation effect which can be recognized with naked eyes from the flocculation of suspension. The long-wavelength absorption band turned dominant when Cys:Cd^{2+} ratio was increased to 1:1, indicating a much serious aggregation of Au-(Cys/Cd) particles therein.

We chose Au-(Cys/Cd) colloids with the Cys:Cd^{2+} ratio of 1:0.5 as the starting material for the subsequent hydrothermal reaction to grow CdS shell. Upon the hydrothermal reaction at 130 °C for 6 h, Cys/Cd complexes, initially attached on the surfaces of Au, decomposed to yield CdS on Au surfaces, resulting in the formation of Au-CdS core−shell nanocrystals. The X-ray diffraction (XRD) pattern of the product shown in Figure S3 of the Supporting Information verifies the growth of hexagonal wurtzite CdS along with fcc Au nanocrystals in the hydrothermal reaction. Figure 1a shows the typical transmission electron microscope (TEM) image of the resulting composite nanocrystals. The apparent contrast between the inner core and the outer shell suggests the existence of core−shell structures. The contrast can be clearly seen in the inset of Figure 1a, from which a shell thickness of about 6 nm is observed. The composition within the composite particles was then examined using TEM-energy dispersive spectrometry (TEM-EDS). The TEM-EDS elemental mapping of Au, Cd and S shown in Figure 1b confirmed the core−shell feature of Au-CdS nanocrystals. Figures 1c and d further show the detailed crystallographic structures of the as-obtained Au-CdS core−shell nanocrystals. In Figure 1c, an HRTEM image taken at the interface of core and shell regions of a single particle, two distinct sets of lattice fringes were revealed. An interlayer spacing of 0.24 nm was observed in the core region, in good agreement with the *d* spacing of the (111) lattice planes of the fcc Au crystal.[16] In the shell region, an interlayer spacing of 0.34 nm was however obtained, complying with the lattice spacing of the (002) planes of the wurtzite CdS.[17] The corresponding electron diffraction pattern, shown in Figure 1d, further verifies the presence of both Au and CdS nanocrystals with two sets of diffraction patterns indexed as fcc Au and wurtzite CdS, respectively. This result, together with those of XRD, HRTEM, and TEM-EDS analyses, confirms the formation of Au-CdS core−shell nanocrystals by using Au-(Cys/Cd) colloids as the starting material in the hydrothermal reaction. It should be noted that the as-synthesized core−shell nanocrystals of Au-CdS retained considerably high dispersity in water, probably coming from the remaining carboxyl groups at their surfaces (see the Supporting Information, Figure S4). Furthermore, CdS-free Au particles or CdS-coated nanocrystals containing multiple Au cores were rarely observed, demonstrating the advantage of the current synthetic approach to obtain core−shell nanocrystals. The success of this work to fabricate core−shell heterostructures was achieved by applying Cys as the trifunctional reagent in the hydrothermal process, instead the lattice parameter relationship between Au and CdS. As shown in Figure S5 of the Supporting Information, a lattice mismatch of 33.3% is observed for the present Au-CdS system, implying no epitaxial relationship exists between Au core and CdS shell.

By controlling the experimental conditions such as the hydrothermal reaction time, the concentration of Cys/Cd complexes and the molar ratio of Cys/Cd to Au-Cit colloids, we were able to modulate the thickness of CdS shell in the range of a few to several tens nanometers. For example, a shell thickness of about 2 nm could be obtained once the hydrothermal reaction was conducted for only 1 h. On the other hand, CdS shell can grow up to 9 nm in thickness by simply raising the concentration of Cys/Cd to 10 mM while keeping the other synthetic conditions fixed. To further shell growth, we increased the molar ratio of Cys/Cd to Au-Cit colloids by increasing the volume of Cys/Cd (10 mM) added into Au-Cit colloids (9 mL, 0.25 mM). Figure 2 reveals the morphological evolution of Au-CdS nanocrystals obtained by employing 10 mM Cys/Cd of four various volumes. We depicted the correlation of Cys/Cd volumes with the resulting CdS shell thickness in Figure S6 of the Supporting Information. With increasing volumes of Cys/Cd added into Au-Cit colloids, there are increasing amount of CdS formed on the surfaces of Au nanoparticles, leading to an extensive growth of CdS shell in the resulting Au-CdS nanocrystals.

Nanosized Au particles exhibit strong SPR absorption at around 520 nm.[18] The position of SPR absorption of Au colloids depends on particle size, shape, as well as the medium

(15) (a) Templeton, A. C.; Pietron, J. J.; Murray, R. W.; Mulvaney, P. *J. Phys. Chem. B* **2000**, *104*, 564. (b) Zhong, Z.; Patskovskyy, S.; Bouvrette, P.; Luong, J. H. T.; Gedanken, A. *J. Phys. Chem. B* **2004**, *108*, 4046.

(16) For bulk fcc Au, $d(111) = 0.2355$ nm from JCPDS 04−0784.

(17) For bulk wurtzite CdS, $d(002) = 0.3367$ nm from JCPDS 06−0314.

(18) Eustis, S.; El-Sayed, M. A. *Chem. Soc. Rev.* **2006**, *35*, 209.

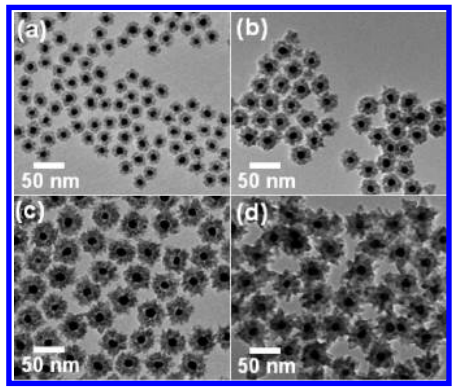

Figure 2. TEM images of Au-CdS nanocrystals prepared by employing 10 mM Cys/Cd of (a) 1, (b) 2, (c) 4, and (d) 8 mL.

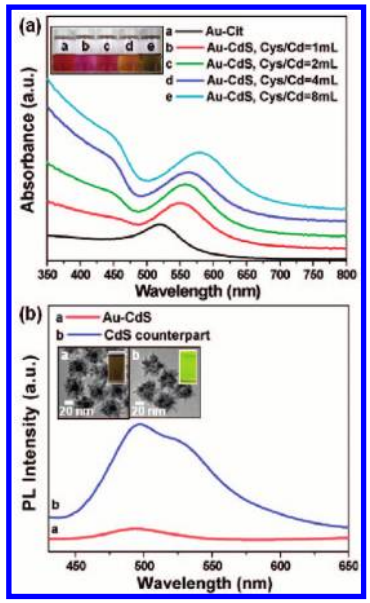

Figure 3. (a) UV−visible absorption spectra of Au-Cit and Au-CdS nanocrystals prepared by employing 10 mM Cys/Cd of various volumes. Inset shows the corresponding solution colors. (b) PL spectra of Au-CdS and CdS counterpart nanocrystals with their solution colors and TEM observations inserted for comparion.

surrounding them.[15,19] For example, coating Au particles with a dielectric leads to a shift in the SPR position. As shown in Figure 3a, the SPR absorption of Au colloids shifted from 520 to 553 nm after the growth of 9 nm thick CdS shell. Such an extent of SPR red-shift was consistent with the theoretical calculation result.[20] The increasing thickness of CdS shell is responsible for the further red-shift in the SPR position of Au. Similar phenomenon was ever observed in Au-SiO_2,[21] Au-SnO_2,[6a] and Au−Fe_3O_4[22] core−shell nanocrystal systems, in which the coverage of shell materials possessing a higher refractive index led to a red-shift in the SPR position of Au. Further growth of shell thickness caused an enhancement in the overall refractive index of the medium surrounding Au, which in turn promoted the dielectric effect and resulted in more pronounced red-shift in the SPR position of Au.

Core−shell nanocrystals of Au-CdS provide an ideal platform to investigate the photoinduced charge transfer property for the metal-semiconductor heterostructures. Note that Au core can serve as an effective electron scavenger for CdS shell. The Fermi level of Au is located at around +0.5V versus NHE, lower in the energetic state than the conduction band of CdS (−1.0 V vs NHE).[23] Consequently, most of the photoexcited free electrons in CdS shell would transfer to Au core, leading to the depletion of free electrons in CdS domain and the subsequent suppression of excitonic emission of CdS. Figure 3b shows the photoluminescence (PL) spectrum of the as-synthesized Au-CdS nanocrystals compared with that of CdS counterpart. CdS counterpart was prepared by treating Au-CdS nanocrystals with KCN to remove Au core, producing hollow structures of CdS (see the Supporting Information Figure S7). The PL spectrum of CdS counterpart exhibited a major emission band at 495 nm and a minor shoulder at 530 nm. The band at 495 nm could be attributed to the typical excitonic band-to-band radiative emission of CdS because of its location near the absorption edge (475 nm, as determined from the absorption spectra of Figure 3a). The shoulder at 530 nm however originated from the trap-state emission.[24] This trap-state emission probably came from the structural defects such as surface states produced in CdS shell during the KCN treatment. As compared to CdS counterpart, a significant quenching in the PL emission of CdS was observed for Au-CdS nanocrystals, indicating the occurrence of charge separation and electron transfer from CdS shell to Au core. This demonstration supported our argument that Au core acts as an effective electron scavenger for CdS shell.

In conclusion, we have developed a facile and reproducible approach for preparing Au-CdS core−shell nanocrystals with controllable shell thickness. The photoinduced charge separation property was demonstrated and revealed in the as-synthesized Au-CdS nanocrystals. The present synthetic route can be readily extended to obtain other sulfide-semiconductor-coated Au nanocrystals such as Au-ZnS (see the Supporting Information, Figure S8).

Acknowledgment. This work was financially supported by the National Science Council of the Republic of China (Taiwan) under Grant NSC-96-2218-E-009-011 and by the National Chiao Tung University under Grant 96W807.

Supporting Information Available: Experimental details, SPR calculation method, XPS spectra, UV−visible spectra, XRD patterns, and TEM images (PDF). This material is available free of charge via the Internet at http://pubs.acs.org.

CM802074J

(19) (a) Njoki, P. N.; Lim, I. S.; Mott, D.; Park, H.-Y.; Khan, B.; Mishra, S.; Sujakumar, R.; Luo, J.; Zhong, C.-J. *J. Phys. Chem. C* **2007**, *111*, 14664. (b) Chen, H.; Kou, X.; Yang, Z.; Ni, W.; Wang, J. *Langmuir* **2008**, *24*, 5233.
(20) The detailed SPR calculation method is descibed in the Supporting Information.
(21) (a) Liz-Marzán, L. M.; Giersig, M.; Mulvaney, P. *Langmuir* **1996**, *12*, 4329. (b) Salgueiriño-Maceira, V.; Caruso, F.; Liz-Marzán, L. M. *J. Phys. Chem. B* **2003**, *107*, 10990.
(22) (a) Shi, W.; Zeng, H.; Sahoo, Y.; Ohulchanskyy, T. Y.; Ding, Y.; Wang, Z. L.; Swihart, M.; Prasad, P. N. *Nano Lett.* **2006**, *6*, 875. (b) Shevchenko, E. V.; Bodnarchuk, M. I.; Kovalenko, M. V.; Talapin, D. V.; Smith, R. K.; Aloni, S.; Heiss, W.; Alivisatos, A. P. *Adv. Mater.* **2008**, DOI: 10.1002/adma.200702994, in press.
(23) Kamat, P. V.; Shanghavi, B. *J. Phys. Chem. B* **1997**, *101*, 7675.
(24) Hsu, Y.-J.; Lu, S.-Y.; Lin, Y.-F. *Chem. Mater.* **2008**, *20*, 2854.